Proceedings of the 20th International Conference on Soil Mechanics and Geotechnical Engineering– Rahman and Jaksa (Eds)

Hierarchical Multiscale SPH (HM-SPH): A new continuum approach to model desiccation cracking in clay soils

Giang D. Nguyen
School of Civil, Environmental & Mining Engineering, University of Adelaide, Australia

Ha H. Bui
Department of Civil Engineering, Monash University, Australia

ABSTRACT: Desiccation cracks are formed by the shrinkage of clay soils due to moisture loss. The presence of cracks can induce significant changes in the mechanical and hydrological properties of soils, which can lead, for example, to damage of lightly loaded structures (e.g., residential houses), shallow-buried structures (e.g., gas and water pipelines), progressive slope/dam failures, cracking in road pavements and the leakage of deep nuclear waste/hazardous gasses from soils. Therefore, understanding the mechanism of desiccation cracking behaviour in clayey soils is vital for dealing with critical issues relevant to a range of applications in numerous disciplines such as geotechnical engineering, transport engineering, mining and resource engineering and soil science. In this paper, we will present our current effort in developing an advanced computational tool to model shrinkage induced desiccation cracking in clay soils. A new computational approach, namely Fracturing SPH Particles, that combines the smoothed particle hydrodynamics (SPH) method and a new size-dependent constitutive framework capable of describing localised failure problems is proposed. The key advantage of this approach is its capability to describe the fracture geometry through a set of Lagrangian particles, which can freely move in the computational space without being confined to a grid system. Since each SPH particle carries its own cohesive fracture process zone, the new approach can bypass the need to represent the fracture's topology and fracture orientation. The direction of crack propagation is, therefore, mainly controlled by local stress conditions and material properties. Furthermore, owing to the size-dependent feature of the constitutive model, the proposed method can naturally capture the crack propagation in clay soils without being influenced by the well-known issue associated with spatial-dependent solutions.

KEYWORDS: Smoothed Particle Hydrodynamics (SPH), fracturing SPH particles, crack propagation, desiccation cracking, clay.

1 INTRODUCTION

Desiccation cracking in clayey soils occurs when the soils lose moisture. It increases hydraulic conductivity and accelerates the evaporation rate of pore water, lowering water retention in soil. As a consequence of decreasing moisture, matrix suction increases and this can induce cracking due to the development of tensile stress that can exceed the cohesion of soils. Desiccation cracking and changes in both mechanical and physical properties have adverse effects on the soils, the environment, and structures (Holland 2012, Shin & Santamarina 2011). The prediction of desiccation cracking is not only practically important but also is computationally challenging.

Desiccation cracking in clay soils is usually complex involving the initiation and propagation of several cracks at the same time, leading to complex three-dimensional cracking patterns. Modelling such complex cracking processes is challenging for existing computational techniques based on the eXtended Finite Element Method (e.g. Mohammadnejad & Khoei 2013, Vahab et al 2019), Strong Discontinuity Approach (e.g. Cazes et al 2016), or mesh fragmentation approach (e.g. Sanchez et al 2014) that have been used for simulating fracture in geomaterials. The challenges lie in the three-dimensional (3D) simultaneous developments of desiccation cracking that involve the initiation, activation/deactivation, branching and coalescence of several cracks, in addition to the large deformation involved that mesh-based techniques may not always be suitable for. Sophisticated computational techniques that have been successfully used for simpler cracking processes in rocks and concrete that usually involve a few two-dimensional cracks cannot be effectively used, given they rely on explicit representation of crack topologies. Allowing cracks to develop at the interfaces between elements (e.g. Sanchez et al 2014) can help capture complex cracking processes but requires sufficiently fine meshes not to restrict the crack orientations. On the other hand, the use of Discrete Element Method in this area has become more popular (e.g. Sima et al 2014, Tran et al, 2021). Its applications are, however, limited to small scale simulations due to high demands on computational resources.

In this paper, we present a continuum-based approach to modelling complex desiccation cracking processes in clayey soils that can overcome limitations of existing computational approaches addressed above. The Smoothed Particle Hydrodynamics (SPH; Gingold & Monaghan 1977) is used as a platform for enhancements to handle multiple cracks that can simultaneously develop and propagate in the soils, given its versatility for several geomechanics applications, including fracture of geomaterials (Bui et al 2008, 2011, 2014; Bui & Nguyen, 2021). Cracks are embedded in SPH particles, thanks to the enrichment of strain field at particle level. This enrichment introduces a length scale to the behavior of the particle, making the behavior size-dependent and naturally overcoming discretization dependent issues due to cracking. Each SPH particle can have its own crack orientation depending on its stress condition and an assembly of several "fracturing SPH particles" will form the topology of a 3D crack. In this sense, the topology of a crack and its 3D propagation is naturally governed by stress conditions and properties at the particle level.

The formulation is presented in the next section, followed by examples to demonstrate the capability and versatility of the proposed approach.

2 FORMULATION

2.1 *Bridging behavior of an SPH particle and the embedded fracture*

Due to high gradient of deformation across the cracking area, generally termed localization zone, the assumption of homogeneous deformation in a Representative Volume Element (RVE) is no longer valid. As a consequence, continuum

mechanics breaks down, requiring enrichments in either numerical methods for the solution of Boundary Value Problems, or constitutive models. The latter, on enriching the constitutive behavior, is adopted and presented here given it is suitable for applications based on SPH. The enrichment of strain and the introduction of cracks at the particle level follow our earlier work on the development of a size-dependent constitutive modelling framework for localized failure (Nguyen et al, 2016; Nguyen & Bui, 2020) and its applications in geomechanics (Le et al 2018; Wang et al 2019; Tran et al 2020).

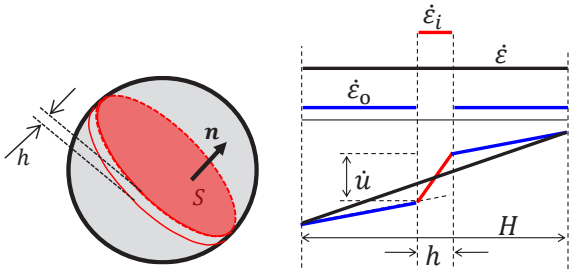

(a) An SPH particle with an embedded localisation band (b) Strain rate and velocity jump across the localisation band

Figure 1. (a) A fracturing SPH particle & (b) one-dimensional illustration of strain rates inside and outside the localization zone.

Consider a particle with an embedded localization zone of width h (Figure 1), for compatibility, the strain rate $\dot{\boldsymbol{\varepsilon}}^{\mathrm{i}}$ inside the localisation zone takes the following form (Figure 1b; Neilsen & Schreyer 1993):

$$\dot{\boldsymbol{\varepsilon}}^{\mathrm{i}} = \dot{\boldsymbol{\varepsilon}}^{\mathrm{o}} + \frac{1}{h}(\mathbf{n} \otimes \dot{\mathbf{u}})^{\mathrm{sym}} = \dot{\boldsymbol{\varepsilon}}^{\mathrm{o}} + \frac{1}{2h}(\mathbf{n} \otimes \dot{\mathbf{u}} + \dot{\mathbf{u}} \otimes \mathbf{n}) \tag{1}$$

The normal vector of the band is denoted as $\mathbf{n}$ and h is the thickness of the localization zone. As can be seen the strain rate $\dot{\boldsymbol{\varepsilon}}^{\mathrm{i}}$ includes homogeneous term $\dot{\boldsymbol{\varepsilon}}^{\mathrm{o}}$ representing the strain rate outside the localization band, and the non-homogeneous term, $\dot{\mathbf{u}} \otimes \mathbf{n}$, generated by the velocity jump $\dot{\mathbf{u}}$ across the localization band. It is noted that pseudo rates are used in the formulation just for the sake of simplicity in the presentation. Given the width h of the localization zone is very small in the case of fracturing processes, the second term in equation (1) is dominant. Therefore we can write:

$$\dot{\boldsymbol{\varepsilon}}^{\mathrm{i}} \approx \frac{1}{h}(\mathbf{n} \otimes \dot{\mathbf{u}})^{\mathrm{sym}} \tag{2}$$

The macro strain rate in this case can be obtained from the homogenization of strain rates inside and outside the localization zone:

$$\dot{\boldsymbol{\varepsilon}} = f\dot{\boldsymbol{\varepsilon}}^{\mathrm{i}} + (1-f)\dot{\boldsymbol{\varepsilon}}^{\mathrm{o}} \tag{3}$$

where $f = h/H$ is the volume fraction of the localization zone. The effective size of the particle is needed and defined as $H = V/S$, where V is the volume of the particle and S the surface area of the localization zone (Figure 1a). In this case, the constitutive behavior of the particle is not based on macro strain $\boldsymbol{\varepsilon}$ and macro stress $\boldsymbol{\sigma}$, but generated from those inside and outside the localization zone, represented by local stresses, $\boldsymbol{\sigma}^{\mathrm{i}}$ and $\boldsymbol{\sigma}^{\mathrm{o}}$, and their corresponding strains, $\dot{\boldsymbol{\varepsilon}}^{\mathrm{i}}$ and $\dot{\boldsymbol{\varepsilon}}^{\mathrm{o}}$.

For the case of a very thin localization band, it has been proved that (Nguyen et al 2012 & 2014; Nguyen & Bui 2020) the macro stress coincides with the stress outside the localization band:

$$\boldsymbol{\sigma} = \boldsymbol{\sigma}^{\mathrm{o}} \tag{4}$$

In this case, the continuity of traction across the boundary of the localization band, $\boldsymbol{\sigma}^{\mathrm{i}} \cdot \boldsymbol{n} = \boldsymbol{\sigma}^{\mathrm{o}} \cdot \boldsymbol{n}$, can be used to obtain the macro stress rate from the macro strain rate, through the constitutive responses inside and outside the localization zone. The rate form of this traction continuity is:

$$\dot{\boldsymbol{\sigma}}^{\mathrm{i}} \cdot \boldsymbol{n} = \dot{\boldsymbol{\sigma}}^{\mathrm{o}} \cdot \boldsymbol{n} \tag{5}$$

The rate forms of constitutive responses inside and outside the localization zone, $\dot{\boldsymbol{\sigma}}^{\mathrm{i}} = \mathbf{D}^{\mathrm{i}} : \dot{\boldsymbol{\varepsilon}}^{\mathrm{i}}$ and $\dot{\boldsymbol{\sigma}}^{\mathrm{o}} = \mathbf{D}^{\mathrm{o}} : \dot{\boldsymbol{\varepsilon}}^{\mathrm{o}}$, can be substituted in the above equation, together with equation (2) and the relationship $\dot{\boldsymbol{\varepsilon}}^{\mathrm{o}} = \left(\dot{\boldsymbol{\varepsilon}} - f\dot{\boldsymbol{\varepsilon}}^{\mathrm{i}}\right)/(1-f)$ obtained from (3), to obtain:

$$\left[\frac{(1-f)}{h}(\boldsymbol{n} \cdot \mathbf{D}^{\mathrm{i}} \cdot \boldsymbol{n}) + \frac{f}{h}(\boldsymbol{n} \cdot \mathbf{D}^{\mathrm{o}} \cdot \boldsymbol{n})\right] \cdot \dot{\mathbf{u}} = (\mathbf{D}^{\mathrm{o}} : \dot{\boldsymbol{\varepsilon}}) \cdot \boldsymbol{n} \tag{6}$$

where $\mathbf{D}^{\mathrm{i}}$ and $\mathbf{D}^{\mathrm{o}}$ are tangent stiffness tensors of the materials inside and outside the localization band, respectively. We consider fracturing processes in a RVE represented by an SPH particle in which the physical width of the localization band is very small compared to the effective size of the particle, e.g. $h \ll H$. In such cases, the stiffness $\mathbf{D}^{\mathrm{o}}$ can be reasonably assumed to be elastic, due to elastic unloading outside the fracture process zone. The first term in the above equation represents the tangent stiffness $\mathbf{K}^{\mathrm{i}}$ of a cohesive-frictional model, and the velocity jump $\dot{\mathbf{u}}$ can be obtained as:

$$\dot{\mathbf{u}} = \underbrace{\left[\mathbf{K}^{\mathrm{i}} + \frac{1}{H}(\boldsymbol{n} \cdot \mathbf{D}^{\mathrm{o}} \cdot \boldsymbol{n})\right]^{-1}}_{\mathbf{C}} \cdot (\mathbf{D}^{\mathrm{o}} : \dot{\boldsymbol{\varepsilon}}) \cdot \boldsymbol{n} \tag{7}$$

The above approach is generic and can be used with any cohesive-frictional model representing the fracture, given in such cases $\dot{\mathbf{t}}^{\mathrm{i}} = \mathbf{K}^{\mathrm{i}} \cdot \dot{\mathbf{u}}$, where $\mathbf{t}^{\mathrm{i}} = \boldsymbol{\sigma}^{\mathrm{i}} \cdot \boldsymbol{n}$ is the traction vector at the interface between the localization band and the surrounding bulk. With $\dot{\mathbf{u}}$ determined, the macro stress rate can be obtained using equations (2-4), as:

$$\dot{\boldsymbol{\sigma}} = \dot{\boldsymbol{\sigma}}^{\mathrm{o}} = \mathbf{D}^{\mathrm{o}} : \left(\dot{\boldsymbol{\varepsilon}} - \frac{1}{H}(\mathbf{n} \otimes \dot{\mathbf{u}})^{\mathrm{sym}}\right) \tag{8}$$

where $f = h/H \approx 0$ has been used. This simplified approach for the case of fracture does not need the definition of the width h of the fracture process zone, given everything has been lumped on the behavior of a cohesive-frictional interface model linking displacement jump with traction. As can be seen, the size of the particle is needed for its constitutive behavior, naturally inducing size effect responses that is essential in modelling localized failure.

For computational purposes, an iterative algorithm is needed to enforce the internal equilibrium at the boundary of the localization zone. The reader can refer to Nguyen & Bui (2020) for details on the algorithm. The implementation in SPH is relatively straightforward given the interface with SPH is through the macro stress – macro strain relationship, and hence everything needed is at particle level. Further details can be found in Tran et al (2020).

2.2 *A cohesive-frictional model*

A cohesive-frictional model based on damage mechanics and plasticity is presented in this Section for the sake of completeness. This model has been used in Nguyen et al (2017) and Tran et al (2020) for modelling fracture in rocks and soils. The traction-displacement jump relationship is written in the local coordinate system of the crack as:

$$\mathbf{t}_c = \begin{bmatrix} t_n \\ t_s \end{bmatrix} = \begin{bmatrix} (1-D)k_n^0(u_n - u_n^p) \\ (1-D)k_s^0(u_s - u_s^p) \end{bmatrix} = \mathbf{K}_c^s \cdot (\mathbf{u}_c - \mathbf{u}_c^p) \quad (9)$$

where t_n and t_s are normal and shear tractions with corresponding displacement jumps u_n and u_s, and their irrecoverable counterparts u_n^p and u_s^p; D is a scalar damage variable; k_n^0 and k_s^0 are elastic stiffness coefficients and $\mathbf{K}_c^s = \text{diag}[(1-D)k_n^0, (1-D)k_s^0]$ is the diagonal secant stiffness tensor.

The yield condition in the local coordinate system is:

$$y = [C^0 F_s^D (C^0 F_s^D - \sigma_t^0 F_n^D \tan\phi)]^2 + t_s^2 \alpha^2 - \left(C^0 F_s^D (C^0 F_s^D - t_n \tan\phi)\right)^2 = 0 \quad (10)$$

where ϕ is the friction angle; σ_t^0 and C^0 are the tensile strength and cohesion, respectively. Function α in the above equation is defined as:

$$\alpha = \sqrt{2C^0 F_s^D \sigma_t^0 F_n^D \tan\phi - (\sigma_t^0 F_n^D \tan\phi)^2} \quad (11)$$

The degradation of tensile strength and cohesion is governed by functions F_n^D and F_s^D, defined as:

$$F_n^D = 1 - \frac{u^p}{u_{nc}^p}; \text{and } F_s^D = 1 - \frac{u^p}{u_{sc}^p} \quad (12)$$

where u_{nc}^p and u_{sc}^p are critical displacement jumps at $D = 1$, and u^p is the accumulated plastic displacement, the increment of which is defined as:

$$\delta u^p = \sqrt{(\delta u_n^p)^2 + (\delta u_s^p)^2} \quad (13)$$

Parameters of the models can be linked with the fracture energies G_I and G_{II} in fracture modes I & II, respectively, as materials properties. The reader can refer to Nguyen et al (2017) and Tran et al (2020) for details on such a model and its corresponding stress return algorithms.

3 NUMERICAL EXAMPLES

The capacity of the proposed approach based on "Fracturing SPH Particles" in handling complex cracking processes involving several cracks is illustrated in this Section, through the simulation of shrinkage induced desiccation cracking in soils. The approach proposed in Sanchez et al (2014) and Bui et al (2015), based on the experimental evidence reported in Rodríguez et al (2007), is adopted for the simulation of shrinkage induced desiccation cracking process. Following this approach, a constant deformation rate, obtained by gradually applying shrinkage stresses to all real SPH particles, while fully fixed boundary is modelled in SPH using virtual particles (Bui et al 2008). The shrinkage stresses are calculated as the product of the increment of the volumetric strain tensor and the elastic Young's modulus (Bui et al 2015). This simplified approach that directly applies shrinkage stresses/strains to the numerical specimen has been commonly used in the literature and is suitable for the simulations of soil desiccation cracking processes. It is adopted in this study given the focus is on simulations of complex desiccation cracking processes, not the hydro-mechanical coupling due to water transport in soils.

3.1 *Cracking of Werribee clay samples*

The experiments on desiccation cracking of Werribee clay samples have been carried out in Monash and details reported in (Amarasiri et al 2011, Tran et al 2020). A long rectangular mould (L=250mm, b=30mm, and h=8, 12, 16mm; Figure 2) are used for samples prepared from dry soil power and mixed with deionized water at gravimetric water content (GWC) of about 80%. To facilitate the crack development, a sandpaper sheet was attached to the base of the mould to increase friction between the soil and the base, and grease was applied to the side boundaries. Due to high friction at the interface between the soil sample and the base, fully fixed boundary condition modelled using virtual particles can be used in SPH model. For samples with thicknesses of 8mm and 12mm, only one particle distance of 0.8mm is used, resulting in 115,810 and 173,715 SPH particles, respectively. Other details on SPH models are in Table 1.

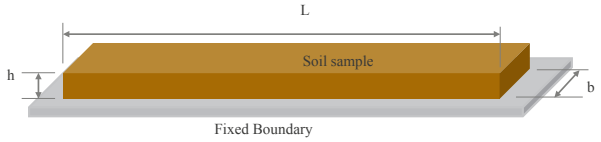

Figure 2. Specimen and boundary condition

Table 1. Detail on SPH models for sample with thickness h=16mm.

Particle distance	0.8mm	0.9mm	1.0mm	1.4mm
No. of real particles	231,620	165,132	120,000	41,349
No. of boundary particles	41,022	33,111	27,648	14,904

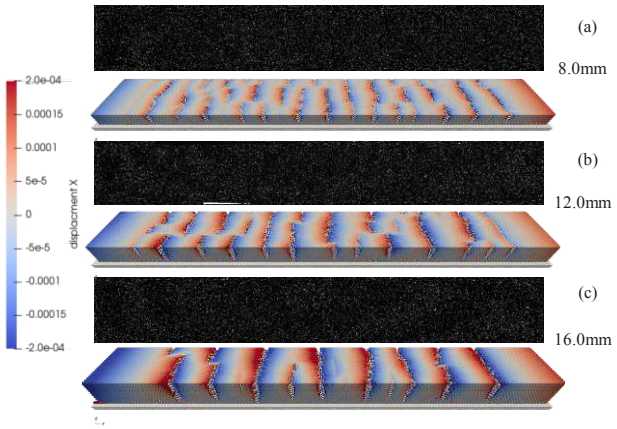

Figure 3. Influence of thickness on cracking pattern.

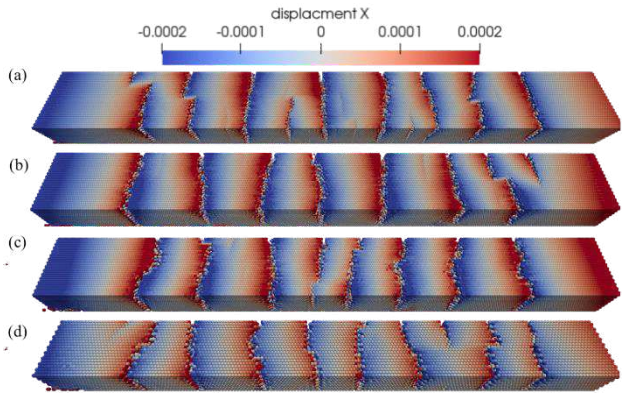

Figure 4. Effects of initial inter-particle distance on fracture pattern (16mm thickness sample): a) 0.8mm; b) 0.9mm; c) 1.0mm; and d) 1.4mm.

For this test, we use friction angle $\phi = 30^o$, Poisson's ratio $\nu = 0.3$. It is assumed that $\sigma_t^0 = C^0$, and fracture energies in both mode I and mode I are the same ($G_I = G_{II}$), while others are

obtained using the following empirical relationships (Tran et al 2020):

$$E = 1256e^{-0.1029GWC} \text{ (MPa)} \quad (10a)$$
$$G_I = 3063e^{-0.1469GWC} \text{ (N/m)} \quad (10b)$$
$$\sigma_t^0 = 5331.9e^{-0.111GWC} \text{ (kPa)} \quad (10c)$$

Figure 3 shows complex cracking pattern obtained from experiments and simulations, for different samples of different thicknesses. The trend in the effects of specimen thickness on cracking pattern can be captured although the density of macro cracks is higher in the SPH simulations than in experiments.

The effects of particle density on the cracking pattern in Figure 4 demonstrate the independence of the numerical solutions with respect to the discretization, thanks to the size dependent feature of the proposed approach. Minor differences in the numerical results when changing the resolution of the spatial discretization are mainly due to the particle oscillation together with the nature of SPH approximation (which induces small changes in different models due to location of particles) and dynamic simulations. Given this is just a preliminary step into modelling complex cracking processes using SPH, further investigation on the sensitivity of cracking patterns with respect to discretization is still needed and will be focused on in the future.

3.1 *Cracking of disc specimens*

Simulations of desiccation cracking of disc specimens of different thicknesses are used to demonstrate the performance of the proposed approach in handling complex cracking processes. The experiments were conducted on circular slurry clay specimens (metallurgical waste) by Rodríguez et al (2007).

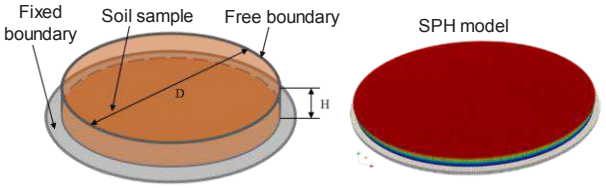

Figure 5. Disc specimens: geometry, dimensions, boundary conditions and SPH model.

The geometry and boundary conditions for the 3D numerical model based on SPH are shown in Figure 3, in which the diameter of the soil specimen is D = 64mm, with three different thicknesses, H=4mm, 8mm and 16mm. The specimen is fully fixed at the bottom and free in all other boundaries (Figure 5). The essential material properties are: Young's modulus E = 4.0MPa, Poisson's Ratio v = 0.2, tensile strength $\sigma_t^0 = 4.0$kPa and fracture energy $G_I = 0.4$ N/m. Further details can be found in Tran (2019).

In the simulation, volumetric shrinkage strains are applied on all real SPH particles. The rate of these strains varies linearly from 2% (at the top layer) to 1% (at the bottom layer), as recommended in a previous study (Tran et al. 2020). The boundary conditions are set to fully fixed at the bottom and fully-free at all other boundaries.

As can be seen seen in Figure 6, the numerical approach based on SPH and Fracturing SPH particles can predict well the development of complex fracture networks, with numerical results in relatively good agreement with their experimental counterparts. In both experiment and simulation, it can be seen that the crack density decreases with the increase of sample thickness. These results are also consistent with the previous SPH approach using different constitutive models (Bui et al. 2015) and FEM-based approach using mesh fragmentation technique (Sanchez et al. 2014). In contrast with mesh-based approach that requires explicit representation of fracture topologies and orientation (Sanchez et al. 2014, Gui et al 2016), macro cracks in this SPH simulations based on Fracturing SPH particles are formed by assemblies of SPH particles, each of which has its own embedded fracture. The evolving stress conditions at particle level governs the initiation and development of these embedded cracks.

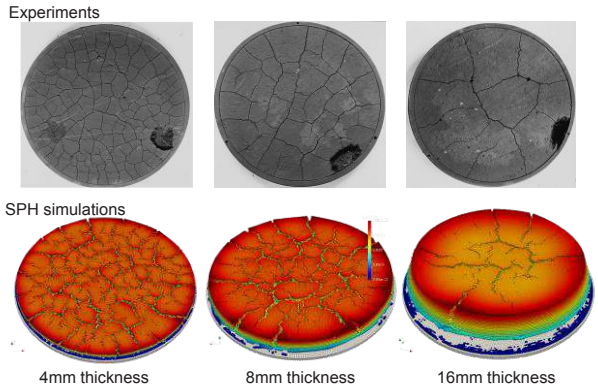

Figure 6. Disc specimens: effect of thickness on fracture pattern.

In the presented SPH simulations fracturing SPH particles naturally move to one side of a macro crack and once fully fractured (damage D=1) the crack opening becomes large enough to stop or minimise the interactions of particles across the crack. Fully fractured SPH particles are then attached to one side of a crack, and each side of an opening crack can then be considered "intact" again with damage being reset to zero to reflect that. This simple approach allows natural developments of cracking processes and minimizes stress locking issues, the resolution of which is usually complex, requiring secondary cracks to be embedded in the structure of the constitutive model (Le et al, 2018).

4 CONCLUSIONS

The proposed approach to embed a fracture in SPH particles allows bridging the behavior of the fracture and that of the SPH particle. The behavior of an SPH particle is governed by the embedded fracture and the elastic zone surrounding it, along with the size of the particle. These Fracturing SPH particles facilitate the modelling of complex fractures in soil desiccation that are challenging for any existing computational approaches, as the explicit representation of fracture topologies of fractures are not needed. Instead, macro cracks are formed by assemblies of Fracturing SPH particles, each of which possesses its own evolving stress state and fracture initiation and evolution. The potential of the approach in handling challenging 3D shrinkage-induced fracture processes in soils, especially in hydro-mechanical coupling due to water transport in soils, will be further investigated in the future. Quantitative validations of numerical results against the experiment (e.g. crack lengths, widths and depths) will be subsequently investigated once the fully coupled hydromechanical model is developed.

5 ACKNOWLEDGEMENTS

The authors gratefully acknowledge support from the Australian Research Council via Discovery Projects DP170103793 (Nguyen & Bui), DP190102779 (Bui & Nguyen), FT200100884 (Bui) and FT140100408 (Nguyen).

6 REFERENCES

Amarasiri A.L., Costa S., Kodikara J.K. 2011. Determination of cohesive properties for mode I fracture from compacted clay beams. *Canadian Geotechnical Journal* 48(8), 1163-1173.

Bui H. H., Fukagawa R., Sako K. & Ohno S. 2008. Lagrangian meshfree particles method (SPH) for large deformation and failure flows of geomaterial using elastic–plastic soil constitutive model. *International Journal for Numerical and Analytical Methods in Geomechanics* 32(12), 1537-1570.

Bui H. H., Kodikara J., Bouazza A., Haque A. & Ranjith P. G. 2014. A novel computational approach for large deformation and post-failure analyses of segmental retaining wall systems. *International Journal for Numerical and Analytical Methods in Geomechanics* 38(13), 1321-1340.

Bui H.H., Fukagawa R., Sako K., Wells J.C. 2011. Slope stability analysis and discontinuous slope failure simulation by elasto-plastic smoothed particle hydrodynamics (SPH). *Géotechnique* 61(7), 565-74.

Bui H.H., Nguyen G.D. 2021. Smoothed particle hydrodynamics (SPH) and its applications in geomechanics: from solid fracture to granular behaviour and multiphase flows in porous media. *Computers and Geotechnics*, in press.

Bui H.H., Nguyen G.D., Kodikara J., Sanchez M. 2015. Soil cracking modelling using the mesh-free SPH method. *12th Australia New Zealand Conference on Geomechanics*.

Cazes F, Meschke G, Zhou M-M. 2016. Strong discontinuity approaches: An algorithm for robust performance and comparative assessment of accuracy. *International Journal of Solids and Structures* 96, 355-379

Gingold R.A., Monaghan J.J. 1977. Smoothed particle hydrodynamics: theory and application to non-spherical stars. *Monthly Notices of the Royal Astronomical Society* 181(3), 375-89.

Gui Y.L., Bui H.H., Kodikara J., Zhang Q.B., Zhao J., Rabczuk T. 2016. Modelling the dynamic failure of brittle rocks using a hybrid continuum-discrete element method with a mixed-mode cohesive fracture model. *International Journal of Impact Engineering* 87, 146-155

Holland M. 2012. Practical guide to diagnosing structural movement in buildings. Ringgold Inc, Portland.

Le L.A., Nguyen G.D., Bui H.H., Sheikh A.H., Kotousov A. 2018. Localised failure mechanism as the basis for constitutive modelling of geomaterials. *International Journal of Engineering Science* 133, 284-310.

Mohammadnejad T, Khoei AR. 2013. Hydro-mechanical modeling of 880 cohesive crack propagation in multiphase porous media using the extended finite element method. *International Journal for Numerical and Analytical Methods in* Geomechanics 37(10), 1247-79.

Neilsen M.K. & Schreyer H.L. 1993. Bifurcations in elastic-plastic materials. *International Journal of Solids and Structures* 30, 521-544.

Nguyen G. D. & Bui H. H. 2020. A thermodynamics- and mechanism-based framework for constitutive models with evolving thickness of localisation band. *International Journal of Solids and Structures* 187, 100–120.

Nguyen G.D., Einav I., Korsunsky A.M., 2012. How to connect two scales of behaviour in constitutive modelling of geomaterials. *Géotechnique Letters* 2, 129-134.

Nguyen G.D., Korsunsky A.M., Einav I., 2014. A constitutive modelling framework featuring two scales of behaviour: Fundamentals and applications to quasi-brittle failure. *Engineering Fracture Mechanics* 115, 221-240.

Nguyen G.D., Nguyen C.T., Nguyen V.P., Bui H.H., Shen L. 2016. A size-dependent constitutive modelling framework for localised failure analysis. *Computational Mechanics* 58, 257-280.

Nguyen N.H.T., Bui H.H., Nguyen G.D., Kodikara J., Arooran S., Jitsangiam P. 2017. A thermodynamics-based cohesive model for discrete element modelling of fracture in cemented materials. *International Journal of Solids and Structures* 117, 159-176.

Rodríguez, R., Sanchez, M., Ledesma, A. & Lloret, A. 2007. Experimental and numerical analysis of desiccation of a mining waste. *Canadian Geotechnical Journal* 44(6), 644-658.

Sanchez M, Manzoli OL, Guimarães LJN. 2014. Modeling 3-D desiccation soil crack networks using a mesh fragmentation technique. *Computers and Geotechnics* 62(0), 27-39.

Shin H, Santamarina JC. 2011. Desiccation cracks in saturated fine-grained soils: particle-level phenomena and effective-stress analysis. Géotechnique 61(11), 961-972.

Sima J., Jiang M. & Zhou C. 2014. Numerical simulation of desiccation cracking in a thin clay layer using 3D discrete element modeling. *Computers and Geotechnics* 56, 168-180.

Tran K.M, Bui H.H., Nguyen G.D. 2021. A hybrid discrete-continuum approach to model hydro-mechanical behaviour of soil during desiccation. *Journal of Geotechnical and Geoenvironmental Engineering*, in press.

Tran T.-H. 2019. A coupled hydro-mechanical SPH framework to model desiccation cracking in clay soils. *PhD Thesis*, Monash University.

Vahab M, Khoei AR, Khalili N. 2019. An X-FEM technique in modeling hydro-fracture interaction with naturally-cemented faults. *Engineering Fracture Mechanics* 212, 269-290.

Wang Y., Bui H.H., Nguyen G.D., Ranjith P.G. 2019. A new SPH-based continuum framework with an embedded fracture process zone for modelling rock fracture. *International Journal of Solids and Structures* 159, 40-57.